sciendo
ISSN 1335-8871
MEASUREMENT SCIENCE REVIEW
Journal homepage: https://content.sciendo.com

Prediction of the Natural Gas Compressibility Factor by using MLP and RBF Artificial Neural Networks

Neven Kanchev, Nikolay Stoyanov*, Georgi Milushev

Department of Electrical Measurements, Technical University of Sofia, Bulgaria, n_stoyanov@tu-sofia.bg

Abstract: The compressibility factor indicates the deviation of the real natural gas from the ideal behavior. It is one of the most important parameters in the natural gas industry. In the present study, two different types of neural networks – multi-layer perceptron (MLP) and radial basis functions (RBF) – were used to predict the compressibility factor *Z* of natural gas. The pressure, temperature, and speed of sound (*SoS*) were chosen as input parameters for the artificial neural network (ANN) models. The training and testing of the MLP-ANN and RBF-ANN were carried out on the basis of 151 days of continuous measurements. Different variants of both types of neural networks were implemented and a comparative analysis of their modeling capabilities was performed. The models developed show a very high prediction accuracy, with the results obtained showing a certain advantage of the RBF-ANN. The comparative analysis was performed on the basis of standard performance indicators such as R^2, root mean square error (*RMSE*), mean square error (*MSE*), mean absolute error (*MAE*). The present study shows an intelligent method implemented in two different variants to determine the compressibility factor of natural gas without the need to use the equation of state.

Keywords: natural gas, compressibility factor, artificial neural network, multi-layer perceptron, radial basis functions

1. INTRODUCTION

The accurate custody transfer of natural gas is a complex metering task that has always been the subject of metrological control under an international standard or a local regulation [6]. The proper selection of equipment and the development of a methodology for billing the metered quantities help to maintain a good relationship between all parties involved in custody transfer.

Natural gas is a complex mixture of different components [10]. Essentially, it consists of a mixture of hydrocarbons (mainly methane) and minimal amounts of non-carbon components such as nitrogen, hydrogen sulfide, carbon dioxide, etc. The physical properties of natural gas are a fundamental issue in the gas industry [18], [5]. Among the most important are the compressibility factor, the calorific value, and the energy parameters as well as the determination of the composition of the gas components.

The compressibility factor is denoted by the symbol *Z* and its value is determined by the equation of state (EOS) with the following expression:

$$z = \frac{V_{real}}{V_{ideal}} = \frac{V \cdot P}{n \cdot R \cdot T}, \quad (1)$$

where V_{real} is the volume at real condition, V_{ideal} is the volume at ideal condition, *R* is the universal gas constant, *n* is the number of moles of the gas, *T* is the absolute temperature, *P* is the absolute pressure, and *V* is the volume of the gas. The values of the coefficient of compressibility of natural gas are required for various engineering tasks such as pipeline design, gas metering and others. There are three ways to determine the values of the compressibility factor – experimental data, EOS, and empirical correlations.

The use of highly sensitive flow measuring devices is very important to ensure a high standard of natural gas distribution systems. The measurement of volume flow is carried out using various measuring instruments, such as ultrasonic-meters [7], turbine-meters [20], and rotary-meters [16]. In addition, the calorific value of the gas is another important parameter, which is calculated from the mole fraction of the individual components of the gas [28], [27]. For this reason, the gas operator must develop a method for converting the measured quantity of natural gas from volume units to energy units using an energy conversion device. The metering task is defined by the operation of several separate devices [13], [4] – flow computer (a volume conversion device); volume flow meter; natural gas chromatograph (a calorific value determination device); pressure transmitter; temperature transmitter.

In contrast to the volume flow measurement, where many different devices can be used to calculate the gas calorific value, the gas chromatograph [3] is most commonly used and preferred over calorimeters [27], [14], which are much simpler in design.

DOI: 10.2478/msr-2025-0001

*Corresponding author: n_stoyanov@tu-sofia.bg (N. Stoyanov)

The process gas chromatograph (PGC) determines the physical composition of the natural gas on a molar basis, but it requires a high level of maintenance, such as the supply of carrier and reference gases and scheduled maintenance. All this makes the PGC an expensive asset, and in most cases the gas operator reduces the installation costs by reducing the installation locations.

The ultrasonic flow meter (USM) is the most widely used and reliable measuring device for industrial purposes. It can provide measurements of the speed of sound (*SoS*) parameter, which is also used for internal operational diagnostics. The *SoS* is a parameter that can be observed not only in the USM, but also in the other blocks of the system, such as the gas chromatograph, the pressure and temperature transmitters. It is influenced by the gas composition, the pressure and temperature, the geometry of the measurement section and the transit time measurement of the flow meter.

In recent years, data-driven approaches have been increasingly used to optimize and predict control systems and processes [25], [24]. These are alternatives to conventional techniques, based on artificial intelligence methods. Among them, artificial neural networks (ANN) are the most preferred models. ANNs have a number of advantages, such as approximation of dependencies and high accuracy in prediction [17], [26]. ANN models are often used to increase the accuracy of flow-meter measurements or to predict the calibration process.

Tianjiao Zhang has developed a convolutional ANN to determine the flow rate, analyzing the arrival time of the signal [29]. Based on deep learning, the constructed one-dimensional (1-D) network was verified with real data received from an USM in a pipeline. Santhosh and Roy created an optimized neural network that realizes adaptability in terms of pipe diameter, liquid density and temperature [22]. The output signal of the measuring device is a frequency that is converted into a voltage using a suitable converter. The implemented network avoids the need for re-calibration when changing different parameters.

A majority of the developed neural networks is based on multi-layer perceptron (MLP) architecture to evaluate the compressibility factor, calorific value and *SoS* of natural gas. Jingya Dong et al. implemented ANN for the evaluation of compressibility factor and *SoS* [8]. An MLP-ANN was created as four different types of training algorithms were used: Gradient Descent, Levenberg-Marquart, Conjugate Gradient Descent, and Bayesian Regularization. A multiple linear regression approach was used to create a model that includes three of the training methods.

An example of how the *SoS* value is dependent on the gas mixture is shown in study [15], in which measurements of natural gas with or without the addition of hydrogen (H_2) were compared. The *SoS* is significantly higher when the hydrogen is part of the natural gas. This offers the possibility of accurately measuring the H_2 content only by using ultrasonic gas flow meters.

The other type of neural network that is very often used successfully for predicting natural gas properties is radial basis functions (RBF)-ANN. They have identical characteristics and properties as MLP-ANN. Mohammad Hadi Shateri et al. [23] developed the Wilcoxon Generalized RBF-ANN to predict the compressibility factor of natural gas. An average relative error of 2.3 % was determined and the results were compared with various empirical correlations and equations of state. Elsayed et al. [9] predicted the compressibility factor based on 5490 datasets containing pseudo-reduced values of pressure and temperature. The study is carried out using RBF-ANN, Support Vector Machine and Functional Network. They obtained the best results for RBF-ANN with 0.99 correlation coefficient and 0.14% average absolute error.

The aim of this article is to investigate two ANN models based on MLP and RBF to predict the compressibility factor *Z* of natural gas. The dataset used includes measurement data from an USM of *SoS*, pressure *P* and temperature *T*. The models are evaluated against the key performance indicators. A comparison was made between the properties of the models created.

2. SUBJECT & METHODS

A. Measurement principle

It is characteristic of gases that ideal conditions are reached when the pressure approaches zero. Under real conditions, gases are characterized by a compressibility factor due to various intermolecular interactions. This parameter indicates the extent to which the real gas differs from the ideal gas at a given value of temperature and pressure. Of the thermodynamic parameters, the compressibility factor is an extremely important and critical parameter. There are numerous scientific studies in the literature based on different methods and correlations to calculate the compressibility factor, such as the Standing and Katz chart, the Dranchuk and Abou-Kassem correlation, etc., each of which has different advantages and disadvantages [19], [1].

Some of the main problems are related to the need for more computation time due to the increased complexity of the method or the increased error values in the data range.

The measurement principle is shown in Fig. 1. The USM operates by measuring the propagation times of ultrasonic pulses emitted with a specific *SoS* between two transducers (Fig. 1). The transducers are installed in a direct path, and both continuously alternate their positions as transmitter and receiver.

The volume flow rate at standard natural gas conditions can be determined using the following equation [16]:

$$Q_S = K_1 \cdot u \cdot A, \tag{2}$$

where Q_S is the volume flow rate of the gas at standard conditions, K_1 is the transforming coefficient, u is the flow velocity determined by USM, and A is the cross-section of the pipeline. The value of K_1 can be determined by the following equation:

$$K_1 = \left(\frac{T_b}{T_f}\right) \cdot \left(\frac{P_f}{P_b}\right) \cdot \left(\frac{1}{Z_f}\right), \tag{3}$$

where *T* stands for the temperature, *P* for the pressure, *Z* for the compressibility factor, and the indices *f* and *b* for the flow or the standard conditions.

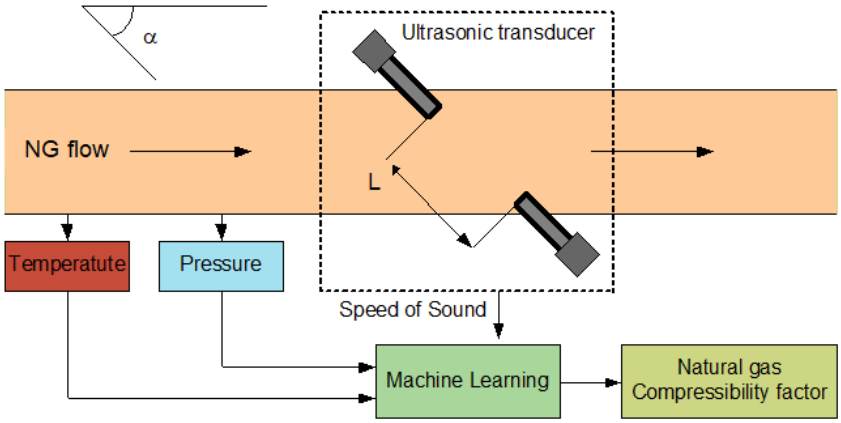

Fig. 1. Ultrasonic flow measurement principle.

The actual *SoS* in the gas under operating conditions can be calculated from the sum of the two measured propagation times (for the forward and opposite direction) of the path:

$$SoS_i = \frac{L_i}{2} \cdot \left(\frac{1}{t_{tr_i}} + \frac{1}{t_{rec_i}}\right), \tag{4}$$

where *SoS* – speed of sound, *L* – path length, t_{tr} – propagation time in the direction of flow, t_{rec} – propagation time against the direction of flow, *i* – current path.

The following formula applies to multipath ultrasonic meters:

$$SoS = \frac{1}{n} \cdot \sum_i^n SoS_i, \tag{5}$$

where n is the number of paths.

The flow velocity can be determined by the following equation:

$$u = \frac{L}{2 \cdot cos\alpha} \cdot \left(\frac{1}{t_{tr}} - \frac{1}{t_{rec}}\right) \tag{6}$$

The compressibility factor is defined in the ISO20765-2 standard. To determine its value, information about the components of the gas is required. Despite the many studies on the estimation of the compressibility factor, there is no general equation that is valid under all conditions. For this reason, alternative methods such as ANN are increasingly used, which offer more possibilities to study the relationships between the variables.

The selection of input parameters for the evaluation of the compressibility factor is based on the well-known relationships and correlations used in traditional methods. The compressibility factor calculated from empirical correlations is characterized by relatively low accuracy and simplified dependencies, which usually include temperature, pressure, and gas composition. The EOS approach has high accuracy because two equations of state have been created specifically for industrial purposes – AGA8 and GERG 2008. In these equations, temperature, pressure, and gas composition data are required to determine the compressibility factor.

In general, both methods, empirical correlations and EOS, require the same input parameters. When a USM is used in the measurement system, it is known from the propagation law of *SoS* that the ultrasonic velocity is different for the various components of the natural gas. For this reason, the *SoS* can be used to evaluate individual components and does not require the use of complex and expensive equipment to assess the composition of the gas.

In the present study, an intelligent approach was developed to determine the compressibility factor without the need for information about the composition of the gas.

B. Multi-layer perceptron model

The ANN is a computer-based tool for parallel processing of information, further classification and forecasting without the knowledge of the functional relationship between the input and output parameters – typical examples are given in [12], [30]. The ANN is executed by interconnected processing units called neurons. They are organized in layers and form the structure of the network. Depending on the location of the neurons, the layers can be divided into three types: input, hidden, and output.

The action of a neuron with the number *j* can be represented by the following equations [11]:

$$y_j' = \sum_{i=1}^n w_{i,j} u_i + b_j, \tag{7}$$

where y_j is the output, w_{ij} is the weight of u_i, and b_j is the bias of the neuron with the number *j*. The activation function *f* is generally non-linear:

$$y_j = f(x)\left[\sum_{i=1}^n w_{i,j} u_i + b_j\right] \tag{8}$$

The current study uses a feed-forward topology based on MLP to predict the compressibility factor *Z* using an ultrasonic flow meter. A Levenberg-Marquardt (LM) and a scaled conjugate gradient descent (SCGD) training algorithm were used to train the network. The structure of the MLP- ANN is shown in Fig. 2.

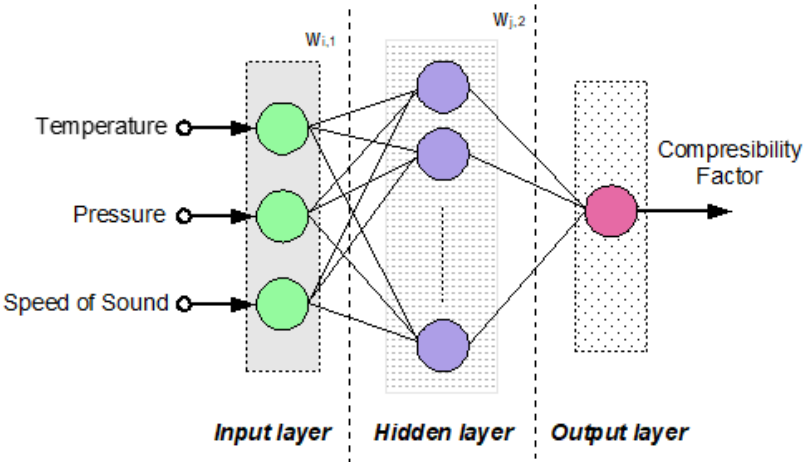

Fig. 2. Schematic diagram of the MLP-ANN.

C. *Radial basis function network design*

RBF networks are widely used due to some important advantages, such as the relatively simple structures and the availability of faster training algorithms [22], [23]. The neural network architecture shown in Fig. 3 includes three layers – an input layer, a hidden layer and an output layer with feed forward algorithm. The RBF-ANN model is implemented with the activation function in the hidden layer depending on the distance between the input signal and a given central point of the neuron. The neurons in this layer usually have Gaussian transfer functions that have the following form [2]:

$$\varphi_i(x) = \exp\left(-\frac{\|x-\mu_i\|^2}{2\sigma_i^2}\right) \tag{9}$$

where φ_i is the nonlinear function of element i, x is the input vector, μ_i is the center of element i, and σ_{i2} is the spread of the Gaussian function in the direction of element i. The form of the output signal of the RBF-ANN is as follows:

$$Y_k(x) = \sum_{i=1}^{m} w_{k,i} \cdot \phi_i(x) + w_{ko} \tag{10}$$

where m is the number of functions, w_{kj} is the weight between basis functions and output, Φ is the nonlinear function of element i, and w_{ko} is the weight of the output layer. The training algorithm of the RBF network is defined by different spread numbers in the interval from 0 to 1.

The MLP-ANN and RBF-ANN studies were performed using MathWorks Matlab software.

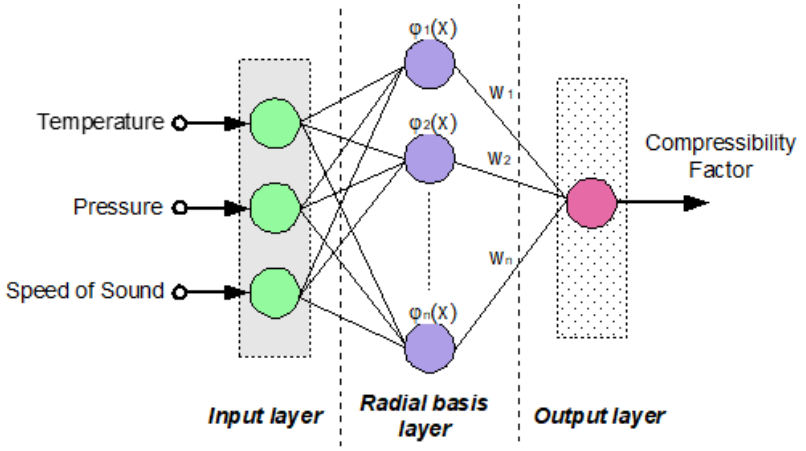

Fig. 3. Schematic diagram of the RBF-ANN.

D. *Data collection*

For the purposes of this research, a package of 151 days of daily average data was collected, processed, and used. The real data set includes 604 values of continuous operation of the measuring devices and was collected from a gas transmission station on the territory of Bulgaria. The measuring equipment includes a USM model SICK Flowsic600-XT Quatro, calibrated measuring range 1.00 ÷ 120.000 m^3/h, relative error 0.2 %, pressure sensor system Rosemount 3051S, relative error 0.035 % and temperature sensor system Rosemount 3144P, relative error 0.25 %. Based on this and using an ANN, it was possible to predict the compressibility factor Z, which is a key parameter for calculating the volume flow at base conditions.

The experimental data for this research was divided into two parts – the first is the training set and comprises 70 % of the observations used to train the MLP and RBF networks. The second set consists of the remaining 30 % of the data for validation. The data forming the training set is necessary for modifying the weights of the connections between the neurons in the structure of the neural network. The validation set is used for the overfitting analysis to obtain an optimal model. This dataset provides an implementation of the "early stopping" technique, which stops the learning of the network, when the validation errors start to increase compared to the training error. This technique overcomes the problems of overfitting and underfitting of ANNs.

E. Performance indicators

The evaluation of the best models is based on standard performance indicators – correlation coefficient R^2, root mean square error (*RMSE*), mean absolute error (*MAE*), and mean square normalized error (*MSNE*) [21]. The correlation coefficient R^2 is estimated in an interval from 0 to 1. Values of R^2 that are closer to 1 indicate a better model. In contrast, the error values for the better models should be close to zero.

$$R^2 = \left(\frac{\sum_{t=1}^{n}(y_t - y_t^M)\cdot(\hat{y}_t - \hat{y}_t^M)}{n \cdot S_{forec} \cdot S_{obs}}\right) \tag{11}$$

$$RMSE = \sqrt{MSE} = \sqrt{\frac{\sum_{t=1}^{n}(y_t - \hat{y}_t)^2}{n}} \tag{12}$$

$$MAE = \frac{1}{n}\sum_{t=1}^{n}|y_t - \hat{y}_t| \tag{13}$$

$$MSNE = \frac{1}{n}\sum_{t=1}^{n}\frac{(y_t - \hat{y}_t)}{(\sum_1^n y_t)\cdot(\sum_1^n \hat{y}_t)} \tag{14}$$

where n is the total number of observations, y_t and $\hat{y}_t$ are the predicted and observed values, y_t^M and $\hat{y}_t^M$ are the means of the predicted and observed values, S_{forec} and S_{obs} are the standard deviation of the predicted and observed values, respectively.

3. RESULTS

A. Multi layer perceptron ANN model

The main problem in the development of the MLP architecture is the allocation of the hidden layers and the number of neurons in these layers. Many attempts have been made to determine the structure of the neural network. The main criterion was to achieve the best value of the correlation coefficient R^2 and the lowest values of *MSNE*, *RMSE*, and *MAE*. Two training algorithms, LM and SCGD, were applied to investigate the number of hidden neurons.

The influence of the number of neurons in the hidden layer for the LM algorithm is shown in Fig. 4. The evaluation is compiled in the form of *MSNE*, *RMSE*, and *MAE* values. The best result of the MLP-ANN structure for the LM algorithm is obtained for 51 neurons in the hidden layer. The effect of the number of hidden neurons for the SCGD learning algorithm is shown in Fig. 5. The best values for *MSNE*, *RMSE*, and *MAE* are obtained for 56 neurons.

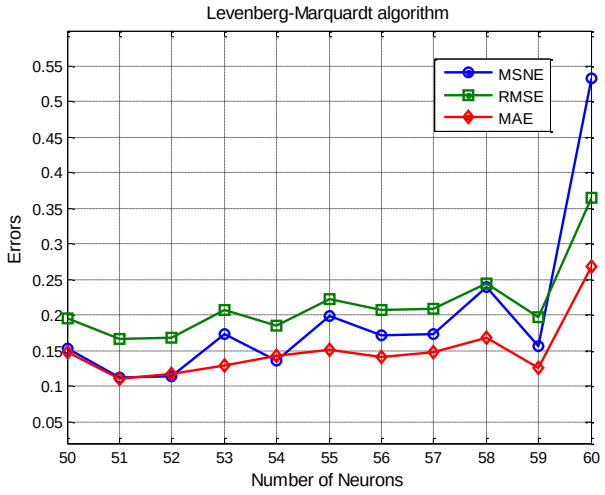

Fig. 4. Effect of the number of hidden neurons of the MLP-ANN for the LM algorithm.

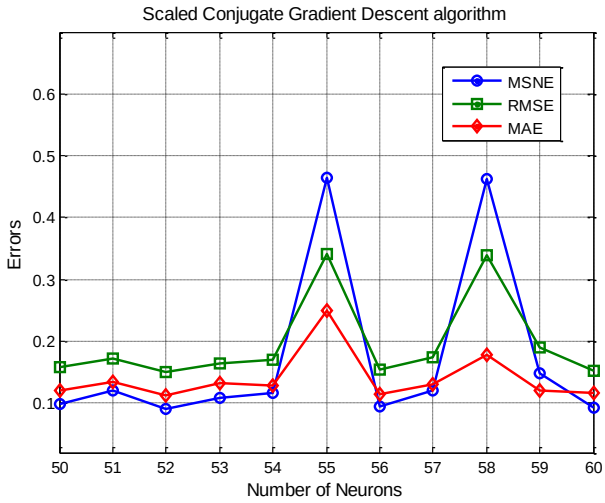

Fig. 5. Effect of the number of hidden neurons of the MLP-ANN for the SCGD algorithm.

A comparative analysis of the LM and SCGD algorithms can be found in Table 1.

Table 1. Comparative analysis of LM and SCGD algorithms.

Algorithm	R^2	*MSNE*	*RMSE*	*MAE*
LM	0.99032	0.0581	0.1206	0.087
SCGD	0.94229	0.0953	0.1543	0.1144

The table shows that the *MSNE* and *RMSE* errors for the LM algorithm are slightly lower compared to the SCGD algorithm, with the correlation coefficient significantly in favor of the first algorithm. MLP-ANN shows the best fit for the optimal number of hidden neurons – 51 for the LM algorithm. The developed three-layer neural network with a 3-51-1 topology and LM algorithm was selected for the next analysis. The input layer includes three neurons (nodes) to which the database of temperature, pressure and *SoS* was applied. The hidden layer comprises 51 neurons and the output layer is represented by 1 node for the output parameter – the compressibility factor.

A linear transfer function of the output neuron of the ANN structure was chosen. The training process is performed with a learning rate of 0.05 and a number of epochs determined after examining the training and validation errors. Different types of activation functions were also tested. In general, the best performance – highest R^2 and lowest error – was obtained for 'tansig' in both the hidden layer and the output neuron. The results are shown in Table 2.

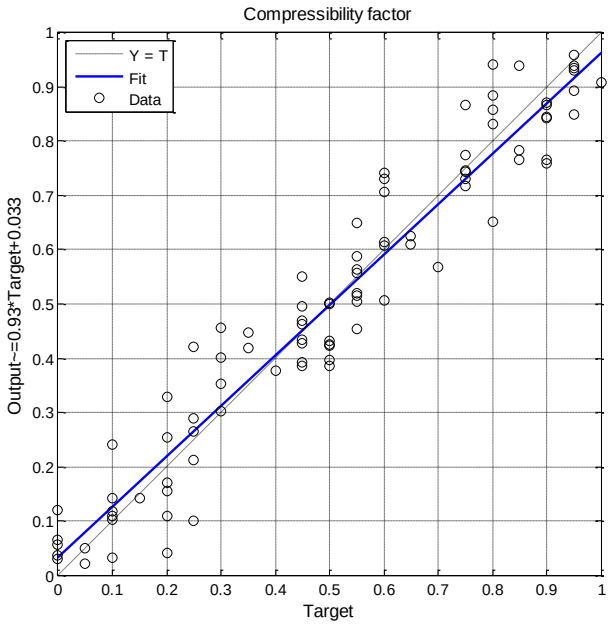

Fig. 6. Scatter plot of predicted values versus observed values for MLP-ANN.

After we ran a simulation with the optimal MLP-ANN architecture, the result of the regression analysis is shown in Fig. 6.

After running the simulation process through the 3-51-1 MLP-ANN, the optimal results obtained are: R^2 = 0.99032; *MSNE* = 0.0581, *RMSE* = 0.1206, *MAE* = 0.087.

The results of the predicted versus observed values after the performed MLP simulation are shown in Fig. 7.

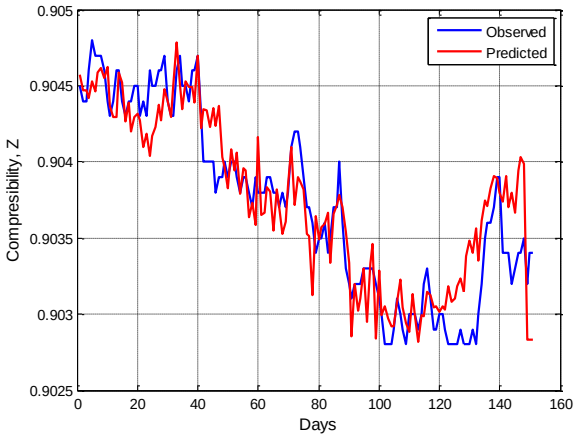

Fig. 7. Plot of predicted values versus observed values for MLP-ANN.

The most appropriate selection of activation functions in the MLP layers was also performed. The tested combinations for the selected variants of the tansig, logsig and purelin functions are listed in Table 2.

The different activation functions tested show that three combinations have identical characteristics (logsig-purelin, tansig-tansig and logsig-tansig), which are close to tansig-purelin without reaching them.

The study of the prediction of the compressibility factor *Z* with MLP shows a very good accuracy of the results obtained, which is comparable to the values obtained by other researchers in this field.

Table 2. Tested combination of activation functions of MLP-ANN.

Activation function hidden layer	Activation function output layer	R^2	*MSNE*	*RMSE*	*MAE*
tansig	tansig	0.99032	0.0581	0.1206	0.087
tansig	purelin	0.99219	0.3866	0.3109	0.2363
logsig	tansig	0.94438	0.1034	0.1607	0.1072
logsig	purelin	0.98062	0.6353	0.3985	0.3117
purelin	tansig	0.82875	0.1136	0.1685	0.1184
logsig	logsig	0.83831	0.2505	0.2502	0.1884
tansig	logsig	0.85305	0.2536	0.2518	0.195
purelin	logsig	0.68672	0.2955	0.2718	0.2067

B. Radial basis function ANN model

An RBF-ANN was developed with three input nodes for temperature, pressure and *SoS* and an output neuron in the third layer for the compressibility factor of the natural gas. The evaluation of the RBF-ANN was based on the same performance indicators: R^2, *RMSE*, *MSNE*, and *MAE*. To obtain an optimal architecture of the network, experiments were performed with different numbers of neurons in the hidden layer and different spread numbers. The analysis includes testing the number of hidden neurons from 10 to 140 and the interval of spread number values between 0.1 ÷ 0.5. The experimental data used to train and test the RBF-ANN are the same as those used for the MLP-ANN. Table 3 shows the results on the influence of the number of neurons in the hidden layer and the different values of spread numbers. The best spread value obtained is *SV* = 0.1 for the number of hidden neurons *HN* = 140 and the performance indicators R^2 = 0.99899, *RMSE* = 0.0135, *MAE* = 0.0075. Fig. 8 and Fig. 9 show a regression plot and a plot of the predicted versus the observed values of the compressibility factor for RBF-ANN.

Table 3. Influence of hidden neurons of RBF-ANN.

Spread value	Neurons	*MSE*	*MSNE*	*RMSE*	*MAE*
0.1	140	0.99899	0.00073	0.0135	0.0075
0.3	140	0.99742	0.0019	0.0215	0.0108
0.5	140	0.99477	0.0038	0.0306	0.014
0.1	130	0.9973	0.0019	0.022	0.0141
0.3	130	0.99257	0.0053	0.0365	0.0181
0.5	130	0.99272	0.0052	0.0361	0.0177
0.1	120	0.9936	0.0046	0.0339	0.02
0.3	120	0.98875	0.0081	0.0449	0.0268
0.5	120	0.98833	0.0084	0.0457	0.0266

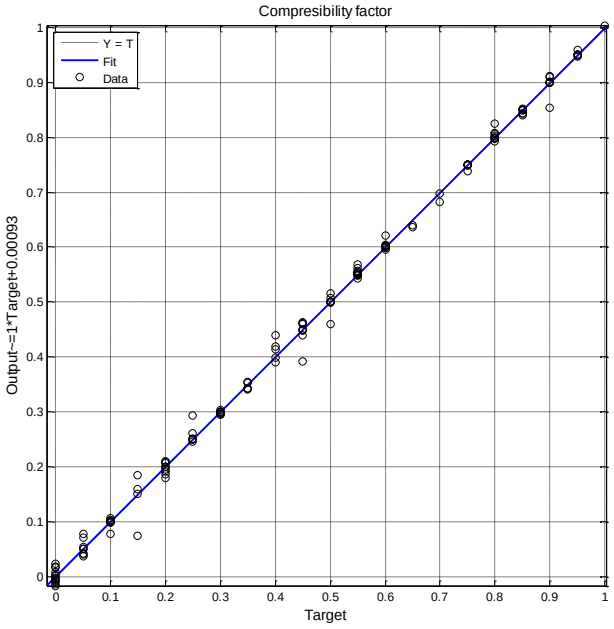

Fig. 8. Scatter plot of predicted values versus observed values for RBF-ANN.

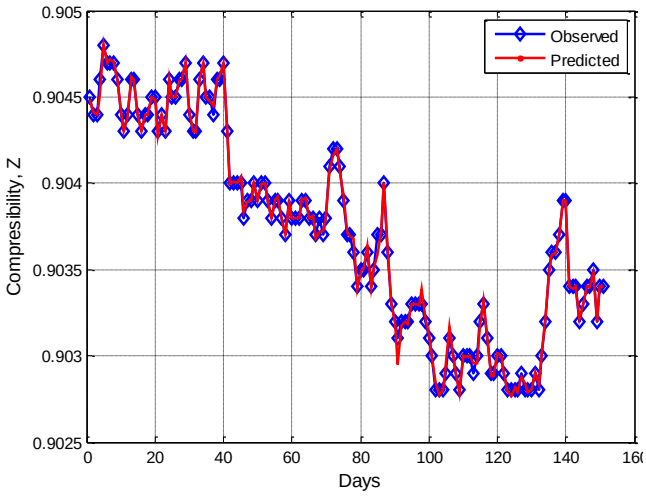

Fig. 9. Plot of predicted values versus observed values for RBF-ANN.

4. Discussion

The aim of this study is to apply a machine-learning approach to predict the compressibility factor of natural gas depending on the data of three input parameters: *SoS*, temperature, and pressure. The intelligent approach used is based on ANN with a hidden layer.

The developed neural networks based on the MLP architecture were evaluated for two learning algorithms: LM and SCGD. The results of the comparative analysis show the better performance of the LM algorithm. This is observed in the error values and the value of the coefficient of determination R^2. The obtained results are in line with other researchers [8] who reported similar values for the parameters R^2 (0.98 ÷ 0.99) and *RMSE* (0.1 ÷ 0.15).

The characteristics of MLP-ANN for different activation functions in the individual layers were investigated. Experiments were performed with different variants of the tansig, purelin and logsig functions. The results obtained show best values for two of the test variants - tansig-tansig and tansig-purelin. For the second combination, R^2 has a higher value, but the error values are significantly higher. Despite the similar characteristics, it can be generally stated that the tansig-tansig combination shows the best behavior of MLP-ANN.

The effectiveness of the modeling process of the compressibility factor of natural gas by MLP-ANN and RBF-ANN was evaluated. The comparison of the models based on the investigated performance indicators R^2, *MSNE*, *RMSE* and *MAE* was performed. The results of the analysis are shown in Table 4.

Table 4. Comparison between MLP and RBF models.

Type ANN	R^2	*MSNE*	*RMSE*	*MAE*
MLP-ANN	0.99032	0.0581	0.1206	0.087
RBF-ANN	0.99899	0.000729	0.0135	0.0075

From the values obtained for the indicators, it can be summarized that they are quite high and very close to similar results obtained by other researchers using the same methods. The correlation coefficient R^2 values are very close to each other. The RBF-ANN model, although with a minimal difference, has a higher value of R^2 = 0.99899 compared to R^2 = 0.99032 obtained by MLP-ANN. The obtained values of *MSNE*, *RMSE* and *MAE* show that the RBF-ANN model has

better properties. The comparative analysis and the values obtained for the coefficient of determination R^2 and errors are identical with the data presented by other researchers [8], [9].

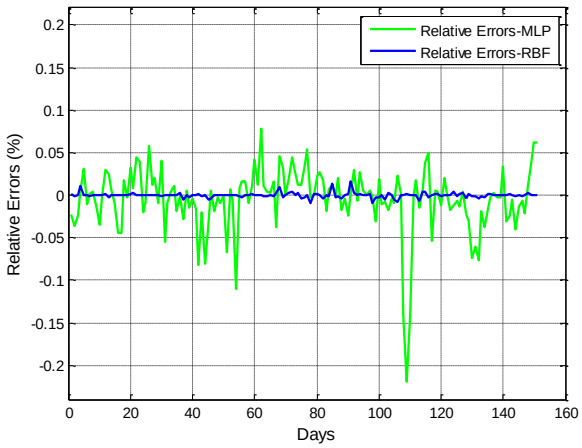

Fig. 10. Comparison of relative errors of the MLP-ANN and the RBF-ANN model.

Fig. 10 shows a comparison of the relative errors (*RE*) for the MLP-ANN and RBF-ANN models. It can be clearly seen that the relative errors for the two ANN models are quite different. The RE values for RBF-ANN are significantly lower compared to those for MLP-ANN for the analyzed area. It is interesting to note that the difference in values is several times greater. From the comparison between Table 4 and Fig. 7, Fig. 9 and Fig. 10, it can be concluded that the correlation coefficients R^2 are very close to each other, while the difference in the *MSNE*, *RMSE*, *MAE* and *RE* errors is significantly in favor of the RBF-ANN model.

5. Conclusion

The current study presents a comparative analysis of two intelligent approaches based on ANN for modeling the compressibility factor of natural gas. Real data from sensors and devices in a gas distribution station on the territory of the Republic of Bulgaria were used for the study. The capabilities of MLP-ANN and RBF-ANN for predicting the *Z*-value are presented so that the results can be used for further calculation of volume flow measurement in the baseline condition.

The ANN approach shows very good abilities and characteristics of the developed models, which can be successfully used for the prediction of the compressibility factor of natural gas. From the results of the comparison of the two methods, it can be concluded that the RBF-ANN has better characteristics. The best values of $R^2 = 0.99899$, $MSNE = 0.000729$, $RMSE = 0.0135$ and $MAE = 0.0075$ for RBF-ANN are similar to the values obtained by other researchers. From the analyses performed, it can be concluded that the better model was obtained by the RBF method.

The graphical interpretation of the comparison between the relative errors for the two models shows that the RBF-ANN model has a clear advantage. The error values *RE* are meny times smaller compared to those of MLP-ANN. The experiments carried out indicate that the RBF-ANN model describes the experimental dataset better, which is based on the better values of all indicators – the correlation coefficient and the errors.

In this study, the compressibility *Z*-factor of natural gas can be calculated from the values of three input variables: temperature, pressure and *SoS*, without the need for chromatographic analysis. The developed ANN is able to realize a high-quality prediction of the *Z*-factor of natural gas with sufficiently high accuracy by using only an ultrasonic flow meter.

Acknowledgment

The authors would like to thank the Research and Development Sector at the Technical University of Sofia for the financial support.

References

[1] Dranchuk, P. M., Abou-Kassem, H. (1975). Calculation of Z factors for natural gases using equations of state. *Journal of Canadian Petroleum Technology*, 14 (03). https://doi.org/10.2118/75-03-03

[2] Ajorkaran, F., Sefidi, A. C. (2019). Application of RBF-ANN in prediction of natural gas density in different operational conditions. *Petroleum Science and Technology*, 37 (22). https://doi.org/10.1080/10916466.2018.1476888

[3] Carotenuto, A., Giovinco, G., Viglietti, B., Vanoli, L. (2005). A new procedure for the determination of calibration curves for a gas chromatograph used in natural gas analysis. *Chemometrics and Intelligent Laboratory Systems*, 75 (2), 209-217. https://doi.org/10.1016/j.chemolab.2004.06.008

[4] Cimerman, F., Jarm, M., Širok, B., Blagojevič, B. (2016). Taking in account measuring errors of volume conversion devices in measuring of the volume of natural gas. *Journal of Mechanical Engineering*, 62 (2), 95-104. https://doi.org/10.5545/sv-jme.2015.2948

[5] Le Corre, O., Loubar, K. (2010). Natural gas: Physical properties and combustion features. In *Natural Gas*. IntechOpen. http://dx.doi.org/10.5772/9823

[6] Coull, C., Spearman, E., Laidlaw, J. (2009). Real life ultrasonic flowmeter verification for upstream custody transfer metering of natural gas. In *XIX IMEKO World Congress: Fundamental and Applied Metrology*. IMEKO, 1276-1281. ISBN 978-963-88410-0-1.

[7] Dell'Isola, M., Cannizzo, M., Diritti, M. (1997). Measurement of high-pressure natural gas flow using ultrasonic flowmeters. *Measurement*, 20 (2), 75-89. https://doi.org/10.1016/S0263-2241(97)00016-X

[8] Dong, J., Song, B., He, F., Xu, Y., Wang, Q., Li, W., Zhang, P. (2023). Research on a hybrid intelligent method for natural gas energy metering. *Sensors*, 23 (14), 6528. https://doi.org/10.3390/s23146528

[9] Elsayed, M. A., Alsabaa, A., Salem, A. M. (2023). Different machine learning approaches to predict gas deviation factor (Z-factor). *Journal of Petroleum and Mining Engineering*, 25 (1), 88-96. https://doi.org/10.21608/jpme.2023.177642.1145

[10] Faramawy, S., Zaki, T., Sakr, A. A.-E. (2016). Natural gas origin, composition, and processing: A review. *Journal of Natural Gas Science and Engineering*, 34, 34-54. https://doi.org/10.1016/j.jngse.2016.06.030

[11] Farzaneh-Gord, M., Mohseni-Gharyehsafa, B., Ebrahimi-Moghadam, A., Jabari-Moghadam, A., Toikka, A., Zvereva, I. (2018). Precise calculation of natural gas sound speed using neural networks: An application in flow meter calibration. *Flow Measurement and Instrumentation*, 64, 90-103. https://doi.org/10.1016/j.flowmeasinst.2018.10.013

[12] Farzaneh-Gord, M., Rahbari, H. R., Mohseni-Gharesafa, B., Toikka, A., Zvereva, I. (2021). Accurate determination of natural gas compressibility factor by measuring temperature, pressure and Joule-Thomson coefficient: Artificial neural network approach. *Journal of Petroleum Science and Engineering*, 202, 108427. https://doi.org/10.1016/j.petrol.2021.108427

[13] Ficco, G., Dell'Isola, M., Vigo, P., Celenza, L. (2015). Uncertainty analysis of energy measurements in natural gas transmission networks. *Flow Measurement and Instrumentation*, 42, 58-68. https://doi.org/10.1016/j.flowmeasinst.2015.01.006

[14] Haloua, F., Ponsard, J.-N., Lartigue, G., Hay, B., Villermaux, C., Foulon, E., Zaréa, M. (2012). Thermal behaviour modelling of a reference calorimeter for natural gas. *International Journal of Thermal Sciences*, 55, 40-47. https://doi.org/10.1016/j.ijthermalsci.2011.12.014

[15] Heinig, D., Starke, E., Ullman, F., Wrath, A. (2022). Measuring hydrogen and hydrogen enriched natural gas flows with ultrasonic flow meters – experiences and perspectives. In *Global Flow Measurement Workshop*. Glasgow, Scotland: TÜV SÜD National Engineering Laboratory.

[16] Bergervoet, J. T. M. (2003). Spin-Offs from the development of rotary gas meters. In *11th Conference on Flow Measurement*. IMEKO, 472-486. ISBN 978-1-63439-896-1.

[17] Kamyab, M., Sampaio Jr., J. H. B, Qanbari, F., Eustes III, A. W. (2010). Using artificial neural networks to estimate the z-factor for natural hydrocarbon gases. *Journal of Petroleum Science and Engineering*, 73 (3-4), 248-257. https://doi.org/10.1016/j.petrol.2010.07.006

[18] Karpash, O., Darvay, I., Karpash, M. (2010). New approach to natural gas quality determination. *Journal of Petroleum Science and Engineering*, 71 (3-4), 133-137. https://doi.org/10.1016/j.petrol.2009.12.012

[19] Katz, D. L., Cornell, D., Vary, J. A., Kobayashi, R., Elenbass, J. R., Poehmann, F. H., Weinaug, C. F. (1959). *Handbook of Natural Gas Engineering*. McGraw-Hill, ISBN 978-0070333840.

[20] López-González, L. M., Sala, J. M., González-Bustamante, J. A., Míguez, J. L. (2006). Modelling and simulation of the dynamic performance of a natural-gas turbine flowmeter. *Applied Energy*, 83 (11), 1222-1234. https://doi.org/10.1016/j.apenergy.2005.12.002

[21] Salehuddin, N. F., Omar, M. B., Ibrahim, R., Bingi, K. (2022). A neural network-based model for predicting Saybolt color of petroleum products. *Sensors*, 22 (7), 2796. https://doi.org/10.3390/s22072796

[22] Santhosh, K. V., Roy, B. K. (2012). An intelligent flow measurement technique using ultrasonic flow meter with optimized neural network. *International Journal of Control and Automation*, 5 (4), 185-196.

[23] Shateri, M. H., Ghorbani, S., Hemmati-Sarapardeh, A., Mohammadi, A. H. (2015). Application of Wilcoxon generalized radial basis function network for prediction of natural gas compressibility factor. *Journal of the Taiwan Institute of Chemical Engineers*, 50, 131-141. https://doi.org/10.1016/j.jtice.2014.12.011

[24] Su, L., Zhao, J., Wang, W. (2021). Hybrid physical and data driven transient modeling for natural gas networks. *Journal of Natural Gas Science and Engineering*, 95, 104146. https://doi.org/10.1016/j.jngse.2021.104146

[25] Su, M., Zhang, Z., Zhu, Y., Zha, D., Wen, W. (2019). Data driven natural gas spot price prediction models using machine learning methods. *Energies*, 12 (9), 1680. https://doi.org/10.3390/en12091680

[26] Szoplik, J., Muchel, P. (2023). Using an artificial neural network model for natural gas compositions forecasting. *Energy*, 263 (D), 126001. https://doi.org/10.1016/j.energy.2022.126001

[27] Ulbig, P., Hoburg, D. (2002). Determination of the calorific value of natural gas by different methods. *Thermochimica Acta*, 382 (1-2), 27-35. https://doi.org/10.1016/S0040-6031(01)00732-8

[28] Villermaux, C., Zarea, M., Haloua, F., Hay, B., Filtz, J.-R. (2006). Measurement of gas calorific value: A new frontier to be reached with an optimised reference gas calorimeter. In *23rd World Gas Conference*. London, UK: International Gas Union (IGU), ISBN 9781604237573.

[29] Zhang, T. (2020). Flow measurement of natural gas in pipeline based on 1D-convolutional neural network. *International Journal of Computational Intelligence Systems*, 13 (1), 1198-1206. https://doi.org/10.2991/ijcis.d.200803.002

[30] Zhang, J., Feng, Q., Zhang, X., Zhang, X., Yuan, N., Wen, S., Wang, S., Zhang, A. (2015). The use of an artificial neural network to estimate natural gas/water interfacial tension. *Fuel*, 157, 28-36. https://doi.org/10.1016/j.fuel.2015.04.057

Received July 18, 2024
Accepted January 8, 2025